Light absorption in hybrid silicon-on-insulator/quantum dot waveguides

Abdoulghafar Omari,[1,2,3,*], Pieter Geiregat,[1,2,3], Dries Van Thourhout,[2,3] and Zeger Hens,[1,2]

[1]*Physics and Chemistry of Nanostructures, Ghent University, B-9000 Ghent, Belgium*
[2]*Center for Nano and Biophotonics (NB Photonics), Ghent University, B-9000 Ghent, Belgium*
[3]*Department of Information Technology, Ghent University - IMEC, B-9000 Ghent, Belgium*
[*]*Abdoulghafar.Omari@UGent.be*

Abstract: We analyze the absorption coefficient of planarized silicon-on-insulator waveguides coated by close packed mono- and multilayers of colloidal PbS/CdS quantum dots (QDs). Experimental data clearly show the influence of the QDs on the waveguide absorbance around 1500 nm, where we find that QDs absorb stronger in thicker layers. To simulate the absorption coefficient of QD functionalized waveguides, the QD layer is replaced by an effective medium with a dielectric function determined by dipolar coupling between neighbouring QDs. Using the host dielectric constant ε_h as an adjustable parameter, excellent agreement with the experimental results is obtained. In this way, the increase in absorption cross section with layer thickness can be traced back to an increasing ε_h. We argue that this reflects the decreasing influence of the surroundings on the ε_h, which therefore evolves from an extrinsic property for monolayers to a more intrinsic film property for multilayers.

OCIS codes: (240.0310) Thin films; (160.4236) Nanomaterials; (160.4760) Optical properties; (230.7370) Waveguides; (230.7390) Waveguides, planar; (310.6860) Thin films, optical properties; (300.1030) Absorption; (260.2065) Effective medium theory; (120.4530) Optical constants.

References and links

1. F. W. Wise, "Lead salt quantum dots: The limit of strong quantum confinement," Accounts of Chemical Research **3,** 773-780 (2000).
2. A. Omari, I. Moreels, F. Masia, W. Langbein, P. Borri, D. Van Thourhout, P. Kockaert, and Z. Hens, "Role of interband and photoinduced absorption in the nonlinear refraction and absorption of resonantly excited PbS quantum dots around 1550 nm," Phys. Rev. B **85,** 115318 (2012).
3. B. De Geyter, A. J. Houtepen, S. Carrillo, P. Geiregat, ' Y. Gao, S. ten Cate, J. M. Schins, D. Van Thourhout, C. Delerue, L. D. A. Siebbeles, and Z. Hens, "Broadband and picosecond intraband absorption in lead-based colloidal quantum dots," ACS Nano **6,** 6067-6074 (2012).
4. J. Heo, Z. Jiang, J. Xu, and P. Bhattacharya, "Coherent and directional emission at 1.55 mu m from PbSe colloidal quantum dot electroluminescent device on silicon," Opt. Express **19,** 26394-26398 (2011), http://www.opticsinfobase.org/oe/abstract.cfm?uri=oe-19-27-26394.
5. N. Daldosso, D. Navarro-Urrios, A. Pitanti, F. Gourbil- leau, R. Rizk, and L. Pavesi, "Erbium and silicon nanocrystals for light amplification," in *Proceedings of IEEE Conference of Lasers and Electro-Optics Society (LEOS)* (Institute of Electrical and Electronics Engineers, Lake Buena Vista, FL , 2007), 933-934.
6. S. Hoogland, V. Sukhovatkin, I. Howard, S. Cauchi, L. Levina, and E. H. Sargent, "A solution-processed 1.53 mu m quantum dot laser with temperature-invariant emission wavelength," Opt. Express **14,** 3273-3281 (2006), http://www.opticsinfobase.org/oe/abstract.cfm?URI=oe-14-8-3273.

#191840 - $15.00 USD Received 6 Jun 2013; revised 25 Aug 2013; accepted 29 Aug 2013; published 24 Sep 2013

7. J. P. Clifford, G. Konstantatos, K. W. Johnston, S. Hoog- land, L. Levina, and E. H. Sargent, "Fast, sensitive and spectrally tuneable colloidal quantum-dot photodetectors," Nature Nanotechnology 4, 40-44 (2009).
8. I. Moreels, B. De Geyter, D. Van Thourhout, and Z. Hens, "Transmission of a quantum-dot-silicon-on-insulator hybrid notch filter," J. Opt. Soc. Am. B **26,** 1243-1247 (2009).
9. A. G. Pattantyus-Abraham, H. Qiao, J. Shan, K. A. Abel, T.-S. Wang, F. C. J. M. van Veggel, and J. F. Young, "Site-selective optical coupling of PbSe nanocrystals to Si-based photonic crystal microcavities," Nano Letters **9,** 2849-2854 (2009).
10. A.Martinez, J. Blasco, P. Sanchis, J. V. Galan, J. Garcia- Ruperez, E. Jordana, P. Gautier, Y. Lebour, S. Hernandez, R. Guider, N. Daldosso, B. Garrido, J. M. Fedeli, L. Pavesi, and J. Marti, "Ultrafast all-optical switching in a silicon-nanocrystal-based silicon slot waveguide at telecom wavelengths," Nano Letters **10,** 1506-1511 (2010).
11. D. V. Talapin, J.-S. Lee, M. V. Kovalenko, and E. V. Shevchenko, "Prospects of colloidal nanocrystals for electronic and optoelectronic applications," Chemical Reviews **110,** 389-458 (2010).
12. J. F. Young, C. Foell, E. Schelew, and Q. Haijun, "Coupling of nanocrystals and photonic crystals for non-linear applications," in *Proceedings of IEEE Conference on Numerical Simulation of Optoelectronic Devices (NUSOD)* (Institute of Electrical and Electronics Engineers, Lake Buena Vista, FL , 2007), 129-130.
13. B. De Geyter, K. Komorowska, E. Brainis, P. Em- plit, P. Geiregat, A. Hassinen, Z. Hens, and D. Van Thourhout, "From fabrication to mode mapping in silicon nitride microdisks with embedded colloidal quantum dots," Appl. Phys. Lett. **101,** 161101 (2012).
14. Z. Hens and I. Moreels, "Light absorption by colloidal semiconductor quantum dots," Journal of Materials Chemistry **22,** 10406-10415 (2012).
15. P. Geiregat, Y. Justo, S. Abe, S. Flamee, and Z. Hens, "Giant and broad-band absorption enhancement in colloidal quantum dot monolayers through dipolar coupling," ACS Nano **7,** 987-993 (2013).
16. See the Appendix section for a thorough discussion of the synthesis, dielectric function, coupled dipole model, experimental and simulated results.
17. J. M. Pietryga, D. J. Werder, D. J. Williams, J. L. Casson, R. D. Schaller, V. I. Klimov, and J. A. Hollingsworth, "Utilizing the lability of lead selenide to produce heterostructured nanocrystals with bright, stable infrared emission," Journal of the American Chemical Society **130,** 4879-4885 (2008).
18. Y. Justo, P. Geiregat, K. Van Hoecke, F. Vanhaecke, C.D. Donega and Z. Hens, "Optical properties of PbS/CdS quantum dots," Journal of Physical Chemistry C, Just Accepted Manuscript.
19. B. De Geyter and Z. Hens, "The absorption coefficient of PbSe/CdSe core/shell colloidal quantum dots," Appl. Phys. Lett. **97,** 161908 (2010).
20. K. Lambert, I. Moreels, D. Van Thourhout, and Z. Hens, "Quantum dot micropatterning on Si," Langmuir **24,** 5961-5966 (2008).
21. Y. Justo, I. Moreels, K. Lambert, and Z. Hens, "Langmuir-Blodgett monolayers of colloidal lead chalcogenide quantum dots: morphology and photoluminescence," Nanotechnology **21,** 295606 (2010).
22. I. Moreels, G. Allan, B. De Geyter, L. Wirtz, C. Delerue, and Z. Hens, "Dielectric function of colloidal lead chalcogenide quantum dots obtained by a Kramers-Kronig analysis of the absorbance spectrum," Phys. Rev. B **81,** 235319 (2010).
23. R. Signorell and A. Bertram, "Physical chemistry of aerosols," Physical chemistry chemical physics : PCCP **11,** 7759-7759 (2009).
24. L. Cademartiri, J. Bertolotti, R. Sapienza, D. S. Wiersma, G. von Freymann, and G. A. Ozin, "Multigram scale, solventless, and diffusion-controlled route to highly monodisperse PbS nanocrystals," J. Phys. Chem. B **110,** 671-673 (2006).
25. A. Neeves and M. Birnboim, "Composite structures for the enhancement of nonlinear-opitcal susceptibility," J. Opt. Soc. Am. B **6,** 787-796 (1989).
26. S. Ninomiya and S. Adachi, "Optical-properties of wurtzite CdS," J. Appl. Phys. **78,** 1183-1190 (1995).
27. A. V. Goncharenko, "Optical properties of core-shell particle composites. I. Linear response," Chem. Phys. Lett. **386,** 25-31 (2004).
28. J. C. De Mello, H. F. Wittmann, and R. H. Friend, "An improved experimental determination of external photoluminescence quantum efficiency," Adv. Mat. **9,** 230232 (1997).
29. R. Quintero-Torres, C. A. Foell, J. Pichaandi, F. C. J. M. van Veggel, and J. F. Young, "Photoluminescence dynamics in solid formulations of colloidal PbSe quantum dots: Three-dimensional versus two-dimensional films," Appl. Phys. Lett. **101,** 121904 (2012).
30. C. A. Foell, E. Schelew, H. Qiao, K. A. Abel, S. Hughes, F. C. J. M. van Veggel, and J. F. Young , "Saturation behaviour of colloidal PbSe quantum dot exciton emission coupled into silicon photonic circuits," Opt. Express **20,** 10453-10469 (2012),http://www.opticsinfobase.org/oe/abstract.cfm?URI=oe-20-10-10453.
31. D. Taillaert, W. Bogaerts, P. Bienstman, T. F. Krauss, P. Van Dale, I. Moerman, S. Verstuyft, K. De Mesel, and R. Baets, "An out-of-plane grating coupler for efficient butt-coupling between compact planar waveguides and single-mode fibers," IEEE J. Quantum Electron. **14,** 949 (2002).

#191840 - $15.00 USD Received 6 Jun 2013; revised 25 Aug 2013; accepted 29 Aug 2013; published 24 Sep 2013

1. Introduction

The optical properties of semiconductor nanocrystals show important deviations from their bulk counterparts. Quantum confinement makes the band gap depend on the nanocrystal dimensions, it reduces the quasi continuous energy bands to a set of discrete energy levels [1] – especially at the band edges – and it leads to a relaxation of selection rules, thus allowing for example light absorption by transitions within an energy band [2, 3]. As a result, the application of semiconductor nanocrystals in optical or photonic devices is widely investigated, using either self-assembled or colloidal quantum dots (QDs) made by epitaxial growth techniques or wet chemical methods, respectively. Compared to self-assembled QDs, colloidal QDs stand out since they can be synthesized in bulk quantities with low size dispersion and may be combined with various materials technology platforms by straightforward solution-based processing methods. Over the last 5 years, their use has been demonstrated in, *e.g.*, light emitting devices, [4], amplifiers [5], lasers [6], displays and photodetectors [7] and they have been combined with integrated photonics platforms based on silicon-on-insulator (SOI) or silicon nitride [8–12].

In device applications, colloidal QDs are mostly deposited as close packed nanocrystal thin films, either within a layered stack [13] or as a surface coating [8] where they interact with the internal or evanescent optical field, respectively. A typical example here involves QDs embedded in a resonator, where the coupling of the QD light emission to the resonator modes eventually leads to lasing [6]. Essential to the development and optimization of such QD-based devices is a proper understanding of the optical field in materials with embedded or surface-coated QD films, where the influence of the QD film on the optical field is properly taken into account. In the literature, it is well known that a dilute dispersion of QDs, either in a liquid or a solid host, can be described as an effective optical medium according to the Maxwell-Garnett effective medium theory in the local field approximation [14]. On the other hand, far fewer studies have addressed the effective medium description of close packed QD films, let alone the experimental investigation and theoretical simulation of the optical properties of hybrid materials containing close packed QD films.

In this letter, we analyze the absorption coefficient of SOI planarized waveguides (PWGs) coated with close-packed mono- and multilayers – generally denoted as *i*-layer with $i = 1, 2, \ldots$ – of PbS/CdS QDs. We retrieve the fingerprint of the QDs in the waveguide absorbance and find that the absorbance per QD increases with the number of QD layers. The experimental data are compared with simulation results, where the QD *i*-layers are described as an effective medium in which the optical properties depend on dipolar coupling between neighboring QDs [15]. Close agreement between the experimental values and the simulation results is obtained using the dielectric constant ε_h of the QD host material as the only adjustable parameter. We find that the increased absorbance in thicker layers makes that a higher value of ε_h is needed to match the simulated and the experimental data. We interpret this as a transition from a regime where the field lines coupling the QDs mainly pass through the surroundings (monolayer case) to a situation where these field lines are mainly confined within the QD stack (thicker multilayers).

2. Experimental

The PbS/CdS core/shell QDs used in this work were synthesized using an established cationic exchange procedure [16, 17]. Core diameter and shell thickness were adjusted to have a band gap absorption at $\approx 1450\,\text{nm}$ (see Fig. 1(a)). In this way, the long wavelength side of the absorption peak covers the $1500 - 1550\,\text{nm}$ bandpass window of the SOI grating couplers, which are used to couple light in and out of the waveguides. This will make the QD absorption well discernible in the measurements. Attempts of measuring the QD absorption of only core PbS QDs on the waveguides, showed a blue shift of the QD wavelength spectrum. This has been observed

#191840 - $15.00 USD Received 6 Jun 2013; revised 25 Aug 2013; accepted 29 Aug 2013; published 24 Sep 2013

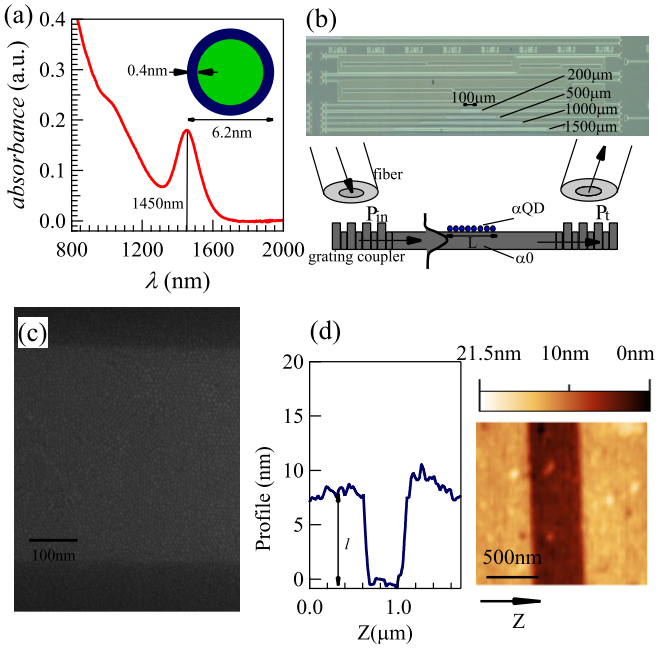

Fig. 1. (a) Absorption spectrum of the PbS/CdS QD used here, as recorded on a dilute QD dispersion in tetrachloroethylene. (b) Optical microscopy image of a sample with planarized waveguides coated by a QD monolayer with various strip lengths and a cartoon representation of the opitcal field coupled from the fiber through the grating in the QD coated PWG. (c) Scanning electron microscopy image of a (topview) PWG coated by a QD monolayer. The resolution is such that the individual QDs coating the waveguide can be discerned. (d) Atomic force microscopy image and cross section of a PWG coated by a QD monolayer, clearly showing the offset (l) between the top surface of the (slightly submerged) PWG and its silica cladding.

previously for PbS QDs deposited on glass substrates [21]. These optically unstable films will hamper a quantitative study of the QD absorption. The growth of the CdS shell allowed for a better passiviation of the PbS core QDs yielding optically stable PbS/CdS particles, which will enable a quantitative comparison between the experimental and theoretical QD absorption. Using the absorption spectrum of the original PbS QDs and the resulting PbS/CdS QDs, core diameter and shell thickness were estimated to be 5.4 and 0.4 nm, respectively [18, 19]. The QDs were locally deposited on the PWGs by combining optical lithography and Langmuir-Blodgett deposition, [20, 21] forming strips of 200, 500, 1000, 1500 μm on otherwise identical waveguides (see Fig. 1(b)). The scanning electron microscopy image shown in Fig. 1(c) is indicative of the close packing and locally hexagonal ordering of the QDs on top of the PWG, while atomic force microscopy imaging reveals that the PWGs are depressed by $5-10$ nm relative to the surrounding silica, with the QD layer conformally following this geometry (see Fig. 1(d)).

The use of QD strips with different interaction length on identical waveguides enables us to quantify the light absorption in the QD functionalized sections of the PWGs, regardless of coupling losses (see Fig. 1(b)). Indeed, denoting the absorption coefficient of a bare and QD coated PWG α_0 and α, respectively, the net absorption coefficient $\alpha_{QD} = \alpha - \alpha_0$ of a QD coated PWG can be derived from the transmitted power P_t through PWGs with different QD

#191840 - $15.00 USD Received 6 Jun 2013; revised 25 Aug 2013; accepted 29 Aug 2013; published 24 Sep 2013

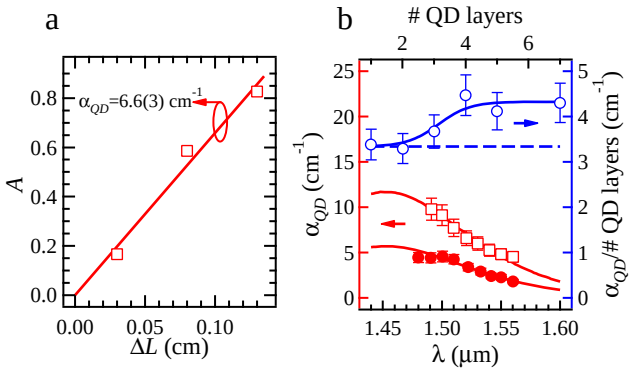

Fig. 2. (a) (open squares) Absorbance A – as defined by Eq. (1) – at 1520 nm as a function of the strip length difference ΔL for PWG coated with a PbS/CdS QD 2-layer strip 500, 1000, and 1500 μm long using the power transmitted through a similar waveguide with a 200 μm QD 2-layer as a reference and (full line) best fit of the data to a line passing through the origin with an indication of the thus obtained absorption coefficient α_{QD}. (b) (red, left and bottom axis) α_{QD} thus determined as a function of wavelength for a (filled circles) QD monolayer and a (open squares) QD 2-layer coated PWG. The full lines represent the absorption spectrum of dispersed PbS/CdS QDs normalized to match the respectively measured absorption coefficients. (blue, right and top axis) α_{QD} per QD layer at 1520 nm. The full line is a guide to the eye and the dashed line indicates the average value obtained for a monolayer and a 2-layer.

strip lengths L. More specifically, using the length of and the power transmitted through one of the QD coated waveguides as a reference, the net waveguide absorbance A reads:

$$A = -\ln \frac{P_t}{P_{t,ref}} = (\alpha - \alpha_0)\left(L - L_{ref}\right) \tag{1}$$

In the determination of A we neglect any contribution of the QD emission to the measured P_t [16].

3. Results and discussion

The net waveguide absorbance is related to the net waveguide loss (dB) as $(10A\log e)$. According to Eq. (1), α_{QD} can be obtained from a plot of A versus the strip length difference $\Delta L = L - L_{ref}$. This is exemplified by Fig. 2(a), which shows A as obtained from measurements on a PWG coated by a PbS/CdS QD 2-layer using the 200 μm strip as a reference. Clearly, A is proportional to ΔL and α_{QD} can thus be obtained as the slope of the best fitting line passing through the origin. The difference between the absorption coefficient thus obtained – $6.6(3)\,\mathrm{cm}^{-1}$ – and the determined $1.8\,\mathrm{dB/cm}$ (*i.e.*, $0.41\,\mathrm{cm}^{-1}$) loss of an uncoated PWG provides a first indication that the QD coating has a strong influence on the waveguide absorbance. This conclusion is further supported by the wavelength dependence of α_{QD}. As shown in Fig. 2(b), the α_{QD} spectrum for a mono- and a 2-layer coating strongly resembles the absorption spectrum of the PbS/CdS QDs used in a dilute tetrachloroethylene dispersion. Similar results are obtained using films consisting of up to 7-layers (see Supplemental Material [16]). Remarkably, we find a higher absorption coefficient per layer for thicker layers (see Fig. 2(b)), meaning that the absorption cross section of a QD in, *e.g.*, a 7-layer is larger than in a monolayer.

#191840 - $15.00 USD Received 6 Jun 2013; revised 25 Aug 2013; accepted 29 Aug 2013; published 24 Sep 2013

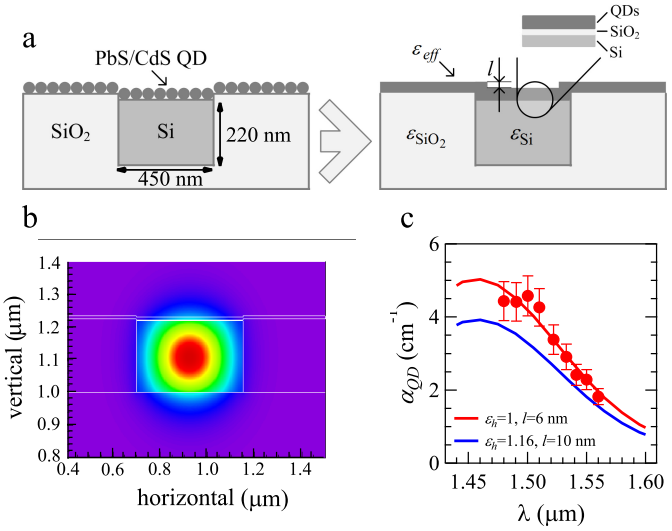

Fig. 3. (a) Cartoon representation of the replacement of the real QD film on top of an SOI planarized waveguide by an effective medium. Indicated are the height difference l between the top surface of the PWG and its silica cladding and the native silica layer in between the PWG top surface and the effective medium representing the QD film. (b) Cross-sectional representation of the simulated electric field for 1520 nm light guided by a PWG coated by a QD monolayer. (c) Comparison of the experimental and simulated α_{QD} absorbance spectrum of a QD coated PWG for two different combinations of l and ε_h.

To compare the experimental α_{QD} with model predictions, we use an approach where the real QD *i*-layer covering the PWG is replaced by an effective medium with a dielectric function ε_{eff} (see Fig. 3(a)). Using the real geometry of the PWG – including the slightly submerged waveguide top surface, coated by a 2 nm thin native silica layer – this enables us to extract a theoretical absorption coefficient $\alpha_{QD,th}$ from the simulated effective refractive index $\tilde{n}_{eff} = n_{eff} + \imath\kappa_{eff}$ of the propagating quasi-TE mode:

$$\alpha_{QD,th} = \frac{4\pi\kappa_{eff}}{\lambda} \tag{2}$$

This approach however requires that the dielectric function of each material or medium involved is known. For silicon and silica, we use typical values at 1520 nm of 3.45 and 1.45, respectively. For ε_{eff}, we build on the recent finding that the absorption cross section of QDs in close-packed monolayers similar to the ones used here can be well described by taking dipolar coupling between neighboring QDs explicitly into account [15]. As shown in the Supplemental Material [16], this coupled dipole model (CDM) also applies to all PbS/CdS QD *i*-layers used in this study. Therefore, the CDM applies for core/shell particles as in [15] only the absorption cross section of core PbS and CdSe core-QD monolayers deposited on glass was studied. Moreover, the study of imaginary part of ε_{eff} through the absorption cross section of QDs in [15] can be extended to yield a generalised expression for ε_{eff} [16]:

$$\varepsilon_{eff} = \varepsilon_h\varepsilon_0\left(1 + \frac{N_s}{L_t}\frac{a_{QD}}{1 - a_{QD}S}\right) \tag{3}$$

Here, N_s is the QD surface density in the layer, L_t is the thickness of the effective layer, a_{QD} is

#191840 - $15.00 USD Received 6 Jun 2013; revised 25 Aug 2013; accepted 29 Aug 2013; published 24 Sep 2013

the polarizability of a single PbS/CdS QD and S is the so-called dipole sum, which sums up the influence of the dipolar field of neighboring QDs on an individual QD in the layer. In general, S is different for fields parallel ($S_{\parallel}$) or perpendicular ($S_{\perp}$) to the QD film. However, since the main field component of the quasi-TE modes in the PWG used here lies parallel to the QD film, only $S_{\parallel}$ – which was analysed experimentally in [15] – is of relevance here.

Opposite from S, which only depends on the position of the particles relative to each other, a_{QD} is a function of ε_h and the dielectric function $\varepsilon_{QD} = \varepsilon_{QD,R} + \imath\varepsilon_{QD,I}$ of the QDs. While we consider ε_h as an adjustable parameter in this study, we use calculated values for $\varepsilon_{QD,R}$ and $\varepsilon_{QD,I}$ [16], taking care that they yield the experimental absorption coefficient spectrum of the QDs in a dilute dispersion while obeying the Kramers-Kronig transformation [22]. Importantly, in this analysis, we assume that the absorption coefficient of the PbS/CdS core/shell QDs at wavelengths shorter than 400 nm can be derived from the bulk dielectric function of PbS and CdS, respectively – as was demonstrated for PbSe/CdSe QDs [19] – and we neglect possible quantization effects in the CdS shell.

Combining the geometry of the PWG cross section and the expression for ε_{eff} – based on the coupled dipole model and the self-consistently determined ε_{QD} – the electric field of the guided optical mode in the PWG can be calculated, resulting in theoretical values for $\tilde{n}_{eff}$ and $\alpha_{QD,th}$. As an example, Fig. 3(b) represents the electric field at a wavelength of 1520 nm for a PWG covered by a QD monolayer as obtained using Fimmwave 3.4 complex mode solver. The figure clearly shows the overlap between the QD film and the evanescent field, which makes that light absorption by the QDs affects κ_{eff} and leads to a non-zero $\alpha_{QD,th}$. The determination of $\alpha_{QD,th}$ would not be possible through a transmission measurement of monolayer coated glass in a spectrophotometer as the absorbance would fall within the noise range. As shown in Fig. 3(c), a close match can be obtained between the simulated and experimental α_{QD} spectrum for a QD monolayer-coated PWG by adjusting ε_h. It should be noted that the ε_h value needed to match the experimental and simulated α_{QD} somewhat depends on the geometry of the PWG. Looking at the AFM cross section of the PWG (see Fig. 1(d)), an exact value of the height difference l between the top surface of the PWG and its silica cladding is hard to determine. Varying l between 6 and 10 nm as extreme cases, we obtain agreement between experiment and simulation for $\varepsilon_h = 1.0$ ($l = 6$ nm) to $\varepsilon_h = 1.16$ ($l = 10$ nm). For QDs capped by oleic acid (ε=2.1 at 2000 nm [23]), both figures are relatively low yet they agree with the $\varepsilon_h = 1.0$ found for PbS and CdSe QD monolayers deposited on glass [15].

The approach as outlined above can be readily extended to simulate α_{QD} for PWG covered by QD i-layers. Using once more ε_h as an adjustable parameter, correspondence between experimental and simulated values can be obtained as shown by the example of a 7-layer in Fig. 4. Importantly, the increasing QD absorption cross section with thicker layers makes that a larger ε_h is needed to fit the simulations to the experimental data when the number of layers increases. As shown in Fig. 4(b), an ε_h in the range of 1.00-1.16 is obtained in the case of a monolayer, whereas values between 1.47 and 1.50 are found for the simulation of the 7-layer using $l = 6$ and $l = 10$ nm, respectively [16]. This demonstrates that in the case of a QD i-layer with i close to one, ε_h is not an intrinsic property of the QD film. Since the field lines that couple neighboring QDs in a monolayer mainly pass through the surroundings, the combined effect of the layers surrounding the QDs – air and native silica on silicon – and the organic ligands separating the QDs will determine ε_h in this case. For thicker layers however, the larger part of these coupling fields remains within the QD film. In that respect, the trend shown in Fig. 4(b) can be interpreted as the progressive evolution of ε_h from an extrinsic value, determined by the layer and its surroundings, in the monolayer case to a value that is an intrinsic property of a QD multilayer.

This results are not only essential for a proper understanding of the optical field in QD mono-

#191840 - $15.00 USD Received 6 Jun 2013; revised 25 Aug 2013; accepted 29 Aug 2013; published 24 Sep 2013

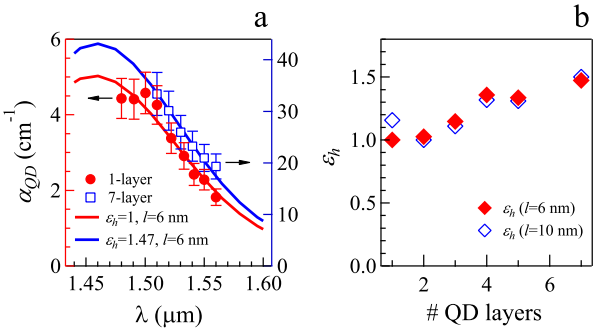

Fig. 4. (a) Comparison of the experimental and simulated α_{QD} spectrum of a PWG coated with (blue) a QD monolayer and (red) a QD seven layer. The respective axis are scaled by a factor of 7 to allow for a direct comparison of the absorbance per number of layers. (b) Evolution of ε_h values needed to match experimental and simulated absorption coefficient calculated for the extreme case of (red) $l = 6$ and (blue) $l = 10$ nm.

layers and the of optical development of QD-based devices, but could have an implication for electronic devices. Thicker QD layers, as outlined above, will allow for more absorption per particle. On the other hand thicker QD layers will hamper charge extraction for photovoltaic or detector devices. In addition, the electric field within a QD layer due to an applied voltage accross the layer will be limited by increasing the layer thickness. This means that the opposing effects of increased absorption and limited electric field will lead to a optimum QD thickness for electronic devices.

4. Conclusion

In conclusion, we have studied light absorption in planarized SOI waveguides functionalized with a top coating of PbS/CdS QD mono- to multilayers. The experimental absorption coefficients can be simulated using an approach where the QD layer is replaced by an effective medium with an effective dielectric function determined by dipolar coupling between neighboring QDs. This approach leaves the host dielectric constant ε_h as the only adjustable parameter and provides a generic scheme to model optical properties of composite materials containing close packed QD films. Using ε_h to match experimental and simulated absorption coefficients, we find that ε_h systematically increases for thicker films. We interpret this as an evolution of ε_h from an extrinsic property, both determined by the QD films and the surrounding layers, to a more intrinsic property of the QD layer. To the best of our knowledge, this is the first demonstration of how ε_h – a typical parameter introduced in effective medium theories – depends on the dimensions of the layer modeled. Our results are essential for the optimization and development of QD-based devices.

5. Appendix

5.1. PbS/CdS synthesis

The PbS QDs were prepared using a procedure as described by [24], where the synthesis conditions were chosen such that oleate capped PbS QDs with a first exciton absorption at 1590 nm – corresponding to a diameter of 6.2 nm – were formed (see blue line in Fig. 5). For the CdS shell growth, a cationic exchange procedure was used, starting from a 5.7μM QD dispersion in toluene. The dispersion was heated to 125°C in a reaction flask placed in an nitrogen atmo-

#191840 - $15.00 USD Received 6 Jun 2013; revised 25 Aug 2013; accepted 29 Aug 2013; published 24 Sep 2013

sphere. Cadmium oleate was added in a 20:1 Cd to Pb ratio. This starts a cationic exchange process in which the outer Pb^{2+} cations are replaced by Cd^{2+} cations, leading to a heterostructure with a PbS core and a CdS shell. The reaction was stopped by quenching with a double amount of ethanol as compared to the reaction volume. After centrifugation and decantation the PbS/CdS Qdots were suspended in toluene. The reduction of the PbS core size by cationic exchange leads to a blueshift of the first exciton absorption. For the PbS/CdS used here, the exciton absorption is shifted to 1450 nm (red line in Fig. 5) leading to particles particles with a total size of 6.2 nm, a shell thickness of 0.4 nm and a size dispersion of 8%.

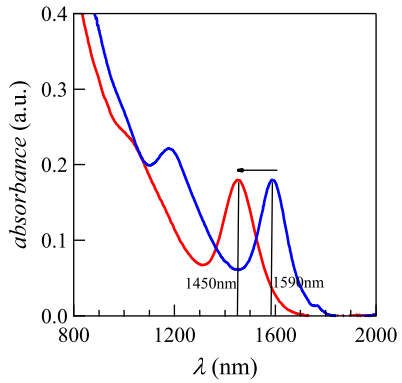

Fig. 5. The QD core shell exciton absorption (red line) shows a blueshift, after cationic exchange procedure, compared with the QD core exciton absorption (blue line).

5.2. *Absorption coefficient spectra for one to seven layer coated PWGs*

We used the method as outlined in the paper to determine the spectrum of the absorption coefficient of PWGs coated with a QD *i*-layer with $i = 1, 2, 3, 4, 5$ and 7. All results are grouped in Fig. 6.

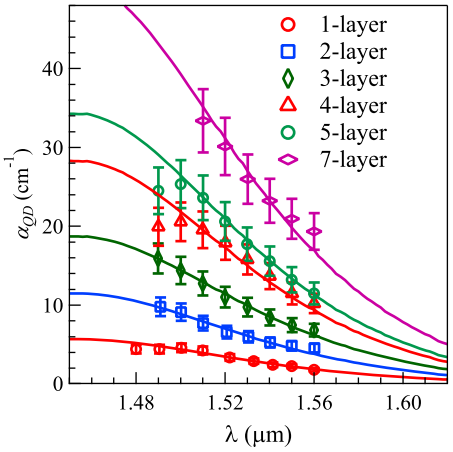

Fig. 6. Experimental α_{QD}, measured as a function of wavelength for a QD monolayer to a QD 7-layer coated PWG. The full lines represent the absorption spectrum of dispersed PbS/CdS QDs normalized to match the respectively measured absorption coefficients.

#191840 - $15.00 USD Received 6 Jun 2013; revised 25 Aug 2013; accepted 29 Aug 2013; published 24 Sep 2013

5.3. *Dielectric constant and polarizability of the PbS/CdS core shell Qdots*

The dielectric response of a core/shell QD ε_{QD} depends on the dielectric function of the core (ε_c) and the shell (ε_{sh}). To determine ε_c and ε_{sh}, we use the iterative matrix inversion method (IMI) as described in [22] for core particles, but we adapt it to the use of a core/shell system. In this method, a self-consistent ε_{QD} is obtained by minimizing the error between the experimentally measured QD intrinsic absorption coefficient ($\mu_{i,exp}$) and the intrinsic absorption coefficient $\mu_{i,th}$ as calculated according to the Mawell-Garnett mixing rule in the local field approximation, while requiring that the real and imaginary part of ε_{QD} are related by the Kramer-Kronig transformation. $\mu_{i,exp}$ can be directly determined from the absorbance A_{susp} of a diluted dispersion of PbS/CdS QDs, where we use tetrachloroethylene (TCE) as the solvent:

$$\mu_{i,exp} = \frac{\ln 10 \times A_{susp}}{f_{susp} L_{cuv}} \tag{4}$$

Here, f_{susp} denotes the volume fraction of the QDs in the suspension, *i.e.*, the ratio between the volume of all suspended QDs and the total volume of the suspension, while L_{cuv} is the cuvette length (1 cm). In the case of PbSe/CdSe core/shell QDs, the correspondence between $\mu_{i,exp}$ and $\mu_{i,th}$ has been confirmed by [19], using the expression of $\mu_{i,th}$ according to [25]:

$$\mu_{i,th} = \frac{2\pi}{\lambda n_s} Im\left(3\varepsilon_s \frac{\varepsilon_{sh}\left[\varepsilon_c(3-2q)+2\varepsilon_{sh}q\right]-\varepsilon_s\left[\varepsilon_c q+\varepsilon_{sh}(3-q)\right]}{\varepsilon_{sh}\left[\varepsilon_c(3-2q)+2\varepsilon_{sh}q\right]+2\varepsilon_s\left[\varepsilon_c q+\varepsilon_{sh}(3-q)\right]}\right) \tag{5}$$

Here, ε_s, n_s denote the dielectric constant and refractive index of the solvent, respectively, while q is ratio of the shell volume to the total core/shell volume. When implementing the procedure outlined above, we have excluded possible quantization effects in the QD shell and used the dielectric constant of bulk CdS [26] for ε_{sh}. The obtained spectral dependence of $\varepsilon_{c,R}$, $\varepsilon_{c,I}$ is shown in Fig. 7(a).

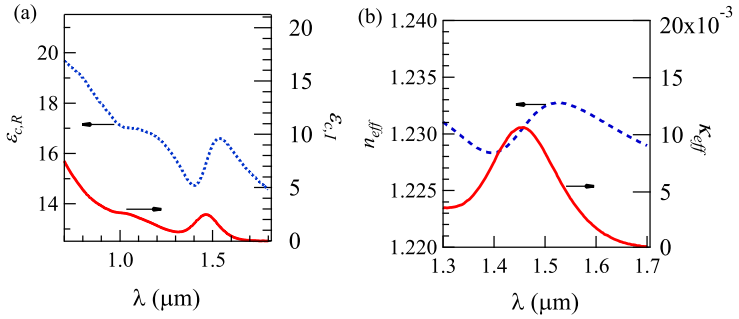

Fig. 7. (a) The dielectric function of the core (PbS) of PbS/CdS Qdots determined using the IMI method for the KK-analysis. Dotted and full line represent respectively $\varepsilon_{c,R}$ and $\varepsilon_{c,I}$. (b) The real part of the complex effective refractive index $\tilde{n}_{eff}$ (dotted line) and the extinction coefficient (full line) extracted from applying the coupled dipole model to the PbS/CdS QD layer.

5.4. *Coupled Dipole Model: Derivation of ε_{eff}*

In the coupled dipole model, we consider a collection of polarizable point particles embedded with a volume density N in a host with permittivity ε_h [15]. We can define an effective dielectric constant ε_{eff} for this composite medium by relating the average dielectric displacement to the average electric field:

#191840 - $15.00 USD Received 6 Jun 2013; revised 25 Aug 2013; accepted 29 Aug 2013; published 24 Sep 2013

$$D = \varepsilon_{eff}E = \varepsilon_0 E + P = \varepsilon_0 E + \varepsilon_0(\varepsilon_h - 1)E + Np_0 \tag{6}$$

In the latter sum, the polarization is split into the contribution of the host and the additional contribution of the dipoles p_0 induced on the point particles. The latter term can be rewritten in terms of the polarizability (a_0) of the point particles and the local electric field E_L that polarizes them:

$$Np_0 = N\varepsilon_0 a_0 E_L \tag{7}$$

Using the expression derived by [27] for spherically symmetrical core/shell particles, a_0 can be expressed as:

$$a_0 = \varepsilon_h \frac{V(\varepsilon_{sh} - \varepsilon_h)\left[\varepsilon_{sh} + (\varepsilon_c - \varepsilon_{sh})\frac{1}{3}(1-p)\right] + p\varepsilon_{sh}(\varepsilon_c - \varepsilon_{sh})}{\left[\varepsilon_{sh} + (\varepsilon_c - \varepsilon_{sh})\frac{1}{3}(1-p)\right]\left[\varepsilon_h + \frac{1}{3}(\varepsilon_{sh} - \varepsilon_h)\right] + p\frac{1}{3}\varepsilon_{sh}(\varepsilon_c - \varepsilon_{sh})} \tag{8}$$

Here, p denotes the ratio of the volume of the core and the volume of the whole core/shell particle.

In the case of a close packed layer, the local field that drives an individual dipole i is the sum of the external field and the field of the neighboring dipoles j:

$$E_{L,i} = E + \sum_{j \neq i} \beta_{i,j} E_{L,j} \tag{9}$$

A crucial element in writing down equation 9 is the assumption that because of symmetry reasons, E_L is the same for all particles:

$$E_L = E + S\varepsilon_0 \frac{a_0}{\varepsilon_h} E_L \tag{10}$$

Here, S is the dipole sum which contains all contributions from the neighboring particles on the local field driving a central particle. For an applied field parallel to the QD film ($S_\parallel$), the dipole sum is given by:

$$S_\parallel = \frac{1}{4\pi} \sum_{j \neq i} \frac{(1 - ikd_{ij})(3\cos^2(\theta_{ij}) - 1))e^{ikd_{ij}}}{d_{ij}^3} + \frac{k^2 \sin^2(\theta_{ij}) e^{ikd_{ij}}}{d_{ij}} \tag{11}$$

To obtain a consistent expression for N in the case of QD i-layers, we determine it as the ratio between the QD surface density in the layer N_s – which is the total number of QDs in the i-layer per unit of surface area – and the thickness L_t attributed to the i-layer. In this study, we take L_t as the product of the number of layers i and the spacing between close-packed planes in an fcc stacking of QDs. With d the QD diameter (6.2 nm) and l_{lig} the thickness of the ligand shell (taken as 1.8 nm), we thus have:

$$L_t = 0.82(d + 2l_{lig}) \times i \approx 8 \times i\,\text{nm} \tag{12}$$

Using this definition of N and L_t, ε_{eff} is obtained as:

$$\varepsilon_{eff} = \varepsilon_h \varepsilon_0 (1 + \frac{N_s}{L_t} \frac{a_{QD}}{1 - a_{QD}S}) \tag{13}$$

In Fig. 7(b), we plot the spectrum of the real and imaginary part of the refractive index as derived from ε_{eff} for a PbS/CdS QD monolayer with a surface density N_s =1.2 $10^{12} \frac{1}{cm^2}$ and taking ε_h =1 and L_t =8 nm.

#191840 - $15.00 USD Received 6 Jun 2013; revised 25 Aug 2013; accepted 29 Aug 2013; published 24 Sep 2013

5.5. *Coupled Dipole Model: Multi-layers*

The use of the coupled dipole model to analyze the effective permittivity of nanocrystal composites was elaborated by [15] for the case of a single component monolayer. Their analysis showed a remarkable absorption enhancement effect absent in other effective medium models for dilute systems, such as the Maxwell-Garnett mixing rule. However, the experimental and theoretical analysis was limited to monolayers of QDs. As shown in Fig. 8(a), the ratio between the absorbance of a QD *i*-layer and the number of layers is in a good approximation constant, which means that the same absorption enhancement as for monolayers holds for *i*-layers. We can thus extend the expression of ε_{eff} that follows from the coupled dipole model to the analysis of QD *i*-layers.

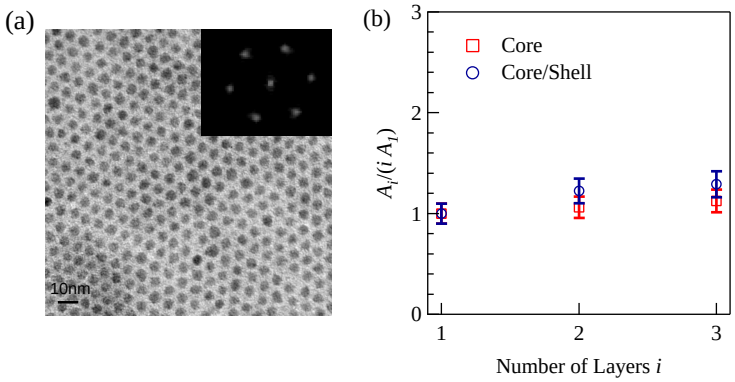

Fig. 8. (a) Monolayer of PbS nanocrystals deposited on TEM grid. Inset : The Fourier image of the monolayer yields a hexagonal diffraction pattern clearly illustrating the strong hexagonal order within the monolayer. (b) The absorbance A_i per layer of *i*-layers of PbS and PbS/CdS QDs normalized relative to the absorbance of a monolayer as a function of the number of layers *i*.

5.6. *Simulated α_{QD} spectrum of the PbS/CdS core shell Qdots*

To simulate the absorption coefficient of the QD functionalized waveguides, the QD layer is replaced by an effective medium with a dielectric function determined by dipolar coupling between neighbouring QDs as outlined above. Using the host dielectric constant ε_h as an adjustable parameter we match the simulated absorption coefficient to the experimental spectrum. As shown in Fig. 9, a good match between both is obtained for all *i*-layers, provided that a larger ε_h is used when the number of layers increases.

#191840 - $15.00 USD Received 6 Jun 2013; revised 25 Aug 2013; accepted 29 Aug 2013; published 24 Sep 2013

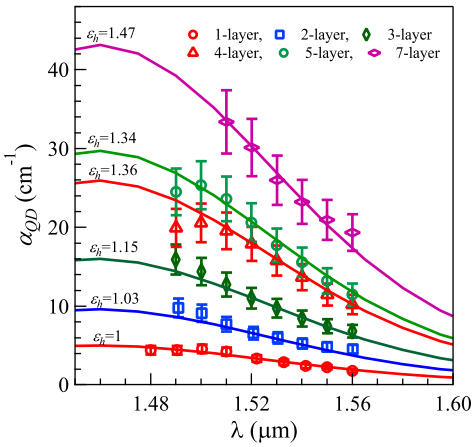

Fig. 9. The full lines represent the absorption spectrum of the simulated α_{QD} spectrum with the needed ε_h values for $l = 6$nm to match the experimental and simulated absorption coefficient. Similar curves where obtained for $l = 10$nm.

5.7. Contribution of the QD PbS/CdS core shell emission to the measured A and P_t

In dispersion, the PbS/CdS QDs used here have a photoluminescence peaking at 1520 nm (see Fig. 10) and a quantum yield of 37%, as determined using an integrating sphere [28]. When deposited on waveguides, part of this luminescence may be coupled to the waveguides, thus raising the transmitted power and lowering the resulting absorption coefficient. In general, the fraction of the absorbed light entering the waveguide in the direction of the detector is determined by the product $QY \times \eta_{coupling}$ of the photoluminescence QY and a coupling factor $\eta_{coupling}$, which is the ratio between the power emitted in the waveguide in one of the two directions to the total power emitted by the QDs. By comparing the transmitted power through waveguides with and without QDs, the net QD absorption coefficient $\alpha - \alpha_0$ is obtained. Clearly, when each QD covering the WGs would re-emit each absorbed photon in the waveguide in the direction of the detector ($QY = 1$, $\eta_{coupling} = 1$), then the QD-emission will fully compensate the QD-absorption and $\alpha - \alpha_0$ would amount to zero. Otherwise, if $QY \times \eta_{coupling} << 1$, the QD-emission contribution to the measured absorbance will be very low and the measured additional waveguide loss can be directly linked to light absorption by the QDs. As mentioned above, the QY of the PbS/CdS QDs in tetrachloroethylene dispersions used here was determined at 0.37. In general, this QY goes down after Langmuir-Blodgett deposition on silicon [29,30], such that the value of 0.37 should be seen as an upper limit. For determining $\eta_{coupling}$, we use an FDTD numerical solver to determine the fraction of the power emitted by a dipole oscillator that is coupled to the waveguide modes. The oscillator is located at a distance of 20 nm from the surface, which should be regarded as an average position of the QD-monolayers relative to the waveguide surface. Along the light propagation direction, the oscillator is put at the center of the waveguide and we find that $\eta_{coupling}$ amounts to 0.15. Here, we accounted for the fact that only half of the emitted light will be collected at one of the waveguide ends and we averaged over the three spatial directions in which the dipole can oscillate. This shows that the emitted light will amounts to, at its best, 5.6% of the absorbed light. This number falls within the ≈10% error of our α_{QD} measurements, and the contribution is therefore discarded.

#191840 - $15.00 USD Received 6 Jun 2013; revised 25 Aug 2013; accepted 29 Aug 2013; published 24 Sep 2013

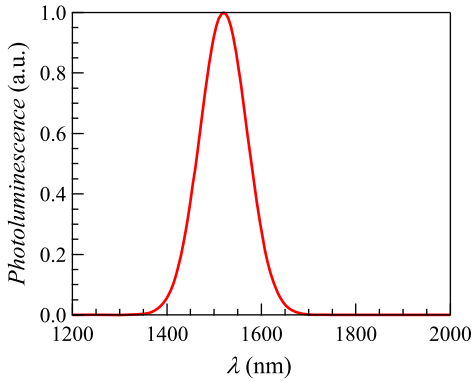

Fig. 10. Photoluminescence spectrum of the PbS/CdS QDs used in this work after excitation at 750 nm. The QDs are dispersed in tetrachloroethylene. The emission peak is at 1520 nm.

Acknowledgments

A.O. acknowledges the Institute for the Promotion of Innovation through Science and Technology in Flanders (IWT-Vlaanderen) for a scholarship. P.G. acknowledges Ghent University for a BOF scholarship. Weiqiang Xie is acknowledged for the FDTD simulations. Z.H. acknowledges the Fund for Scientific Research Flanders (FWO-Vlaanderen) for a research grant (project nr. G.0760.12). Z.H. and D.V.T. acknowledge the Belgian Science Policy Office for funding this research (IAP 7.35, photonics@be).